



CHORUS

This is the accepted manuscript made available via CHORUS. The article has been published as:

Optimal Unambiguous Discrimination of Pure Quantum States

János A. Bergou, Ulrike Futschik, and Edgar Feldman

Phys. Rev. Lett. **108**, 250502 — Published 21 June 2012

DOI: [10.1103/PhysRevLett.108.250502](https://doi.org/10.1103/PhysRevLett.108.250502)

Optimal unambiguous discrimination of pure quantum states

János A. Bergou¹, Ulrike Futschik¹, and Edgar Feldman²

¹*Department of Physics and Astronomy, CUNY Hunter College, 695 Park Avenue, New York, NY 10065*

²*Department of Mathematics, CUNY Graduate Center, 365 Fifth Avenue, New York, NY 10016*

(Dated: March 20, 2012)

A complete geometric view is presented for the optimal unambiguous discrimination among $N > 2$ pure states. A single intuitive picture contains all aspects of the problem: linear independence of the states, positivity of the detection operators, and a graphic method for finding and classifying the optimal solutions. The method is illustrated on the example of three states. We show that the problem depends on the phases of the complex inner products only through an invariant combination, the Berry phase ϕ , and present complete analytical results for $\phi = 0$ and $\phi = \pi$. The optimal solution exhibits full permutational symmetry and is single-valued for a large range of parameters. However, for $\phi = 0$ it can be bi-valued: beyond a critical value of the parameters a second, less symmetric solution becomes optimal. The bifurcation is analogous to a second-order symmetry-breaking phase transition. We conclude with a discussion of the unambiguous discrimination of $N > 3$ states.

PACS numbers: 03.67-a, 03.65.Ta, 42.50.-p

In quantum information and quantum computing the information carriers are quantum systems and information is encoded in their state [1]. Determining the state of a system is, therefore, a fundamental task in quantum information processing.

Quantum state discrimination is one of the methods frequently employed for this purpose and deals with the following problem [2]. Given a quantum system that was prepared in one of $N \geq 2$ known quantum states $\{|\psi_i\rangle | i = 1, \dots, N\}$, but we don't know which, we wish to identify the state of the system as well as allowed by the laws of quantum mechanics. If the possible states are mutually orthogonal this is straightforward: detectors set up along these orthogonal directions will unambiguously identify the states. However, if the states are not mutually orthogonal the problem is highly nontrivial and optimization with respect to some reasonable criteria leads to complex measurement strategies often involving generalized measurements. Finding the optimum measurement strategy is the subject of state discrimination.

Unambiguous discrimination (UD) is one such strategy. In UD errors are not permitted at the expense of allowing an inconclusive measurement outcome to occur. If the input is a system in one of the N states, the measurement will produce one of $N + 1$ outcomes, $0, \dots, N$. If the output is $i > 0$, corresponding to success, then the input was $|\psi_i\rangle$, and if the output is 0, corresponding to failure, then we learn nothing about the input. Since no error is permitted, we will never receive an output of $j \neq i$ if the input was $|\psi_i\rangle$ ($i, j > 0$).

The optimal measurement, which minimizes the probability of the inconclusive outcome, is known for $N = 2$ [3–6]. For $N > 2$ a general result states that UD is possible *iff* the states are linearly independent [7] but the optimal solution is known for special cases only. For general N , these include the solution for equally probably symmetric states [8], a recasting of UD as a semidefinite programming (SPD) problem with numerical results for

symmetric states and geometrically uniform states in [9], and a quantification of linear independence and explicit solution for equidistant states [10].

All other works address the $N = 3$ case: a detailed study of the geometry and topology of the detection operators and numerical examples [11], and explicit solution for the case when the inner products are positive and two or all three are equal [12]. The SPD approach was developed further in [13] where, although no explicit results were given, the solution for real and positive inner products was implicitly obtained. An incomplete geometrical method was introduced in [14] and further explicit solutions were given for the case when one of the overlaps is zero, and for real and positive overlaps. Most recently, [15] appeared with partially overlapping results for real states which is a special case of the $\phi = 0$ and $\phi = \pi$ case, considered here. The connection to Berry's phase, the possibility of a symmetry breaking phase transition and the geometric view remained unnoticed, however.

Optimal UD for $N > 2$ *arbitrary* states remains one of the longest standing open problems in quantum information. Here we develop a complete and intuitive geometric picture that encompasses all aspects of the problem: linear independence of the states, positivity of the detection operators, and a graphic method for finding and classifying the optimal solutions.

To begin, we assume, with no loss of generality, the minimal representation: the N pure states span an N dimensional Hilbert space \mathcal{H} . Since we want $N + 1$ measurement outcomes in an N dimensional Hilbert space, the measurement will be described by a POVM (positive-operator-valued measure). The task is to find the POVM which minimizes the probability of failure.

The POVM elements associated with success are $\Pi_i \geq 0$ for $i > 0$. The probability of success is given by $p_i = \langle \psi_i | \Pi_i | \psi_i \rangle$, and the no-error condition implies $\langle \psi_i | \Pi_j | \psi_i \rangle = 0$ for $j \neq i$. The Π_i 's are constructed as follows. Let \mathcal{S}_i be the subspace spanned by $\{|\psi_j\rangle\}$ for all $j \neq i$ and \mathcal{K}_i the

orthogonal complement, called kernel, such that $\mathcal{S}_i \oplus \mathcal{K}_i = \mathcal{H}$. For UD to be possible, the kernels must be non-empty, so each one is at least a one-dimensional subspace. In addition, to be able to discriminate each of the N states, no two kernels can be identical. Thus, there must be N different, non-empty kernels in an N dimensional Hilbert space. Hence, each one is precisely one-dimensional and together they span the entire Hilbert space \mathcal{H} . Let P_i be the projector onto \mathcal{K}_i . Then $\Pi_i = a_i P_i \geq 0$, $0 \leq a_i \leq 1$, satisfies the requirements for all $i > 0$.

The operator $\Pi_0 = I - \sum_{i=1}^N \Pi_i$ corresponds to failure. The individual failure probabilities are $q_i = 1 - p_i = \langle \psi_i | \Pi_0 | \psi_i \rangle$ and $I = \sum_{i=1}^N \Pi_i + \Pi_0$, because the alternatives represented by the POVM exhaust all possibilities.

The *a priori* probability that the input is $|\psi_i\rangle$ is η_i ($i = 1, \dots, N$ and $\sum \eta_i = 1$). Then the net average success probability is $P = \sum_{i=1}^N \eta_i p_i$ and, accordingly, the total failure probability, $Q = 1 - P$, is given by

$$Q = \sum_i \eta_i q_i. \quad (1)$$

In the optimum UD strategy Q is at its minimum.

The detection operators must be positive, in order to generate positive probabilities. The Π_i 's are positive by construction for $i \geq 1$, so it is sufficient to require $\Pi_0 = I - \sum_{i=1}^N \Pi_i \geq 0$. Linear independence of the states and positivity of the detection operators represent the two constraints for the optimization of (1).

The first step towards a complete geometric view is to visualize the condition of linear independence (LI) of the states. For easy display we assume $N = 3$. The states, $\{|\psi_1\rangle, |\psi_2\rangle, |\psi_3\rangle\}$, have complex overlaps denoted by $\langle \psi_1 | \psi_2 \rangle = s_3 e^{i\phi_3}$, and two more by cyclic permutation of the indexes ($0 \leq s_i \leq 1$). Let us introduce

$$r_1 = \frac{s_1}{s_2 s_3}, \quad r_2 = \frac{s_2}{s_3 s_1}, \quad r_3 = \frac{s_3}{s_1 s_2}. \quad (2)$$

In order to quantify linear independence, we construct the Gram matrix G of the state vectors, $G_{ij} = \langle \psi_i | \psi_j \rangle$ for $i, j = 1, 2, 3$. The determinant, $\det(G)$, is the square of the volume of the parallelepiped spanned by the three vectors. If the volume is zero, the vectors lie in a plane. Thus, the LI condition is simply $\det(G) > 0$, [16]. In terms of the $\{r_i\}$ parameters the condition reads as

$$r_1 r_2 r_3 - r_1 - r_2 - r_3 + 2 \cos \phi > 0. \quad (3)$$

Here we also introduced the invariant phase, $\phi = \phi_1 + \phi_2 + \phi_3$, also called the geometric phase. It corresponds to a phase deficiency associated with a closed path in parameter space ($1 \rightarrow 2 \rightarrow 3 \rightarrow 1$), so it is the Berry phase for the UD problem [17, 18]. If we replace the states $|\psi_i\rangle$ by equivalent states $e^{i\theta_i} |\psi_i\rangle$ we get the same Berry phase and Gram determinant. The parameters r_i and ϕ describe the states up to unitary equivalence.

Equality in (3), for a fixed value of ϕ , defines a smooth surface in the positive octant of the r_1, r_2 and r_3 space. LI states correspond to points above the surface, thus they form a convex set. Points on the surface describe linearly dependent states. Points below the surface are impossible. The boundary surface as well as the convex set of permissible LI states are displayed in Fig. 1.

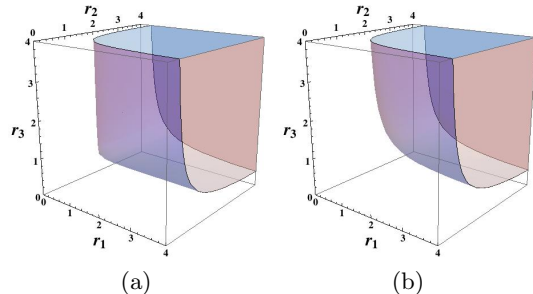


FIG. 1: The convex set of linearly independent states for a) $\phi = 0$ and b) $\phi = \pi/4$.

Let us next turn our attention to the positivity of Π_0 . Because of linear independence, the states that we want to discriminate form a (non-orthogonal) basis. In this basis the diagonal elements of $C_{jk} = \langle \psi_j | \Pi_0 | \psi_k \rangle$ are the failure probabilities, $\{q_i\}$, and the off-diagonal elements are identical to those of G . The non-negativity of Π_0 yields the constraint $\det(C) \geq 0$ and the diagonal sub-determinants of C , Δ_{ij} , are also non-negative, $\Delta_{ij} = q_i q_j - s_k^2 \geq 0$. Again, these conditions and their geometric view become particularly simple in terms of the scaled failure probabilities, $\tilde{q}_i = r_i q_i \leq r_i$ where the inequality follows from $q_i \leq 1$. In terms of the scaled variables the non-negativity conditions are independent of the overlaps and we have $\tilde{\Delta}_{ij} = \tilde{q}_i \tilde{q}_j - 1 \geq 0$ for $i \neq j$, while the main constraint, $\det C \geq 0$ only depends on the Berry phase,

$$\tilde{\Delta} = \tilde{q}_1 \tilde{q}_2 \tilde{q}_3 - \tilde{q}_1 - \tilde{q}_2 - \tilde{q}_3 + 2 \cos \phi \geq 0. \quad (4)$$

The similarity to Eq. (3) is striking. In fact, the substitution $r_i \leftrightarrow \tilde{q}_i$ makes (3) and (4) identical. With a corresponding relabeling of the axes, Fig. 1 also displays the scaled failure probabilities allowed by $\Pi_0 \geq 0$.

For a fixed set of three states, i.e. for a fixed point r_1, r_2, r_3 above the hyperbolic boundary surface in Fig. 1, the condition $0 \leq \tilde{q}_i \leq r_i$ determines a box bounded by the coordinate planes and by the planes $\tilde{q}_i = r_i$. The box and the condition $\tilde{\Delta} \geq 0$ are shown together in Fig. 2a. The intersection of the box with the region allowed by $\tilde{\Delta} \geq 0$ determines the *feasible set* K , shown in Fig. 2b. Every point $\tilde{q} = (\tilde{q}_1, \tilde{q}_2, \tilde{q}_3)$ in K can be realized by some, in general suboptimal, measurement. The geometric construction of the *set* K is displayed in Fig. 2.

To complete the geometric approach we now show how to find the optimal solution within the *feasible set*. We will see that the optimal solution has to lie on the hyperbolic boundary surface of K , hence satisfies $\tilde{\Delta}(\tilde{q}) = 0$. In

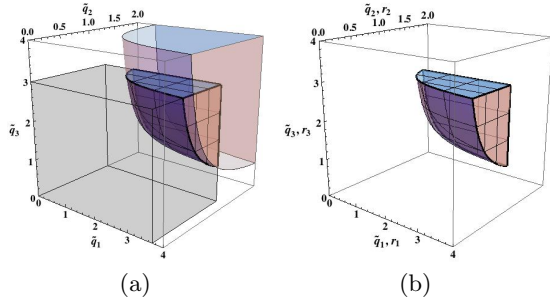


FIG. 2: a) The intersection between the set $\tilde{\Delta}(\tilde{q}_1, \tilde{q}_2, \tilde{q}_3) \geq 0$ and the box $0 \leq \tilde{q}_i \leq r_i$ defines a subset K which contains all admissible values of \tilde{q} . b) The strongly convex subset K . The surface with $\tilde{\Delta}(\tilde{q}) = 0$ is a candidate for the optimal failure probability. Here, $\{r_1, r_2, r_3\} = \{3.7, 1.3, 3\}$ and $\phi = \pi/4$.

order to locate it we now look at the total failure probability Q ($0 \leq Q \leq 1$), expressed in scaled variables,

$$Q = \sum_{i=1}^3 \eta_i \frac{\tilde{q}_i}{r_i}. \quad (5)$$

Eq. (5) represents a family of planes, parametrized by Q in the first octant of the \tilde{q} space. Their normal vector is $\mathbf{N} = (\eta_1/r_1, \eta_2/r_2, \eta_3/r_3)$. For a given Q , the corresponding plane meets the \tilde{q}_i axis at Qr_i/η_i . The full geometric optimization is shown in Fig. 3.

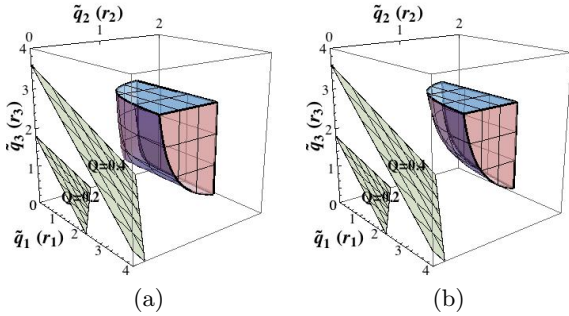


FIG. 3: The tilted triangles are the planes corresponding to the average failure probability, Eq. (5), in the first octant of the $\{\tilde{q}_i\}$ space, for $Q = 0.2$ and $Q = 0.4$, $\eta_i = 1/3$, $\{r_1, r_2, r_3\} = \{3.7, 1.3, 3\}$. Also depicted is the feasible set K of failure probabilities for a) $\phi = 0$ and b) $\phi = \pi/4$.

If we start with the plane $Q = 0$ through the origin then increasing Q will parallel translate it in \tilde{q} space along \mathbf{N} . It meets K for the first time at a unique point $\tilde{q}_{opt} = (\tilde{q}_{1,opt}, \tilde{q}_{2,opt}, \tilde{q}_{3,opt})$ because K is strongly convex. $Q(\tilde{q}_{opt})$ is clearly the minimum value of Q allowed by LI and positivity, Eqs. (3) and (4). Therefore, \tilde{q}_{opt} is the optimal solution and we just completed our geometric approach of finding it. It should be noted that the points on the hyperbolic boundary of K are regular points, the tangent plane is well defined with one notable exception. For $\phi = 0$ the apex (point closest to the origin) is singular. There is a set of tangent planes whose normal vector

is within a cone. If the Q -plane, Eq. (5) has its normal vector within this cone, it will touch the boundary of K at the apex. Thus, for $\phi = 0$ the apex is the optimal solution for a broad range of parameters while for all other values of ϕ the apex is just a regular point.

Let us classify the possible solutions in three categories. *Interior point solution:* \tilde{q}_{opt} is an interior point of the boundary of K . Then all $\tilde{q}_{i,opt} < r_i$ and all three states can be discriminated. *Edge solutions:* \tilde{q}_{opt} lies on one of the edges of K , say $\tilde{q}_{i,opt} = r_i$. Then $q_i = 1$ and we cannot discriminate $|\psi_i\rangle$ but we can discriminate the other two states. The POVM element Π_0 , corresponding to failure, must contain the full $|\psi_i\rangle\langle\psi_i|$ projector. *Vertex solution:* \tilde{q}_{opt} is one of the vertices, say $\tilde{q}_{i,opt} = r_i$ and $\tilde{q}_{j,opt} = r_j$, $i \neq j$. Then we cannot discriminate $|\psi_i\rangle$ and $|\psi_j\rangle$. Π_0 is the full projector on the subspace of $|\psi_i\rangle$ and $|\psi_j\rangle$. This is the worst case scenario, so at least one out of three states can always be resolved.

One of the strengths of the geometric view and the associated graphic method for finding the optimum solution is that it easily lends itself to a complete analytical treatment of the problem. At the optimal point, \tilde{q}_{opt} , the plane $Q = Q(\tilde{q}_{opt})$ is tangent to the surface $\tilde{\Delta}(\tilde{q}) = 0$ in the box $0 \leq \tilde{q}_i \leq r_i$. Calculating the gradient of the plane and the boundary surface and making them equal yield a set of algebraic equations to find \tilde{q}_{opt} ,

$$z_3(\tilde{q}_1\tilde{q}_2 - 1)^2 = z_2|\tilde{q}_1 - e^{i\phi}|^2 = z_1|\tilde{q}_2 - e^{i\phi}|^2 \quad (6)$$

where $z_i = r_i/\eta_i$. This leads in general to a sixth degree equation which can be solved numerically. However, we will illustrate the nature of the optimal solution when $\phi = 0$ and $\phi = \pi$, where computation greatly simplifies.

We start with $\phi = 0$. There are two kinds of solutions. For the first set $\tilde{\Delta}(\tilde{q}_{opt}) = 0$, $\tilde{\Delta}_{i,j}(\tilde{q}_{opt}) = 0$ and $\tilde{q}_{i,opt} < r_i$ for all i . It is easy to show that $\tilde{q}_{opt} = (1, 1, 1)$, or

$$q_i^{(1)} = \frac{s_j s_k}{s_i} \quad \text{for } i \neq j \neq k \quad \text{and } s_i > 0. \quad (7)$$

If all the q_i are less than one, then

$$Q_{opt}^{(1)} = \eta_1 \frac{s_2 s_3}{s_1} + \eta_2 \frac{s_3 s_1}{s_2} + \eta_3 \frac{s_1 s_2}{s_3}. \quad (8)$$

These solutions correspond to the apex of the boundary surface $\tilde{\Delta}(\tilde{q}_1, \tilde{q}_2, \tilde{q}_3) = 0$.

For the second set of solutions $\tilde{\Delta}(\tilde{q}_{opt}) = 0$ but $\tilde{\Delta}_{i,j}(\tilde{q}_{opt}) > 0$. We solve Eq. (6) for \tilde{q}_k and have

$$q_{i(j)}^{(2)} = \frac{\sqrt{\eta_k} s_j^{(i)} - \sqrt{\eta_j^{(i)}} s_k}{\sqrt{\eta_{i(j)}}}, \quad q_k^{(2)} = \frac{\sqrt{\eta_j} s_i + \sqrt{\eta_i} s_j}{\sqrt{\eta_k}} \quad (9)$$

if $\sqrt{\eta_j} s_i + \sqrt{\eta_i} s_j \leq \sqrt{\eta_k}$ and $i \neq j \neq k$. The sub-determinants lead to the following condition

$$\frac{\sqrt{\eta_k}}{s_k} \geq \frac{\sqrt{\eta_i}}{s_i} + \frac{\sqrt{\eta_j}}{s_j}. \quad (10)$$

If all the $q_i < 1$, then

$$Q_{opt}^{(2)} = 2(\sqrt{\eta_i \eta_k} s_j + \sqrt{\eta_j \eta_k} s_i - \sqrt{\eta_i \eta_j} s_k). \quad (11)$$

Finally, $\phi = \pi$ directly leads to the solution

$$q_i^{(3)} = \frac{\sqrt{\eta_j} s_k + \sqrt{\eta_k} s_j}{\sqrt{\eta_i}} \quad \text{if} \quad \sqrt{\eta_j} s_k + \sqrt{\eta_k} s_j \leq \sqrt{\eta_i} \quad (12)$$

and $q_i = 1$ otherwise for $i \neq j \neq k$. If all the $q_i < 1$, then

$$Q_{opt}^{(3)} = 2(\sqrt{\eta_1 \eta_2} s_3 + \sqrt{\eta_1 \eta_3} s_2 + \sqrt{\eta_2 \eta_3} s_1), \quad (13)$$

which is a direct extension of the two states results [6].

Over the range of admissible values of s_3 we have the two solutions for $\phi = 0$, $Q_{opt}^{(1)}$ and $Q_{opt}^{(2)}$. We display their behavior in Fig. 4 for the case of equal *a priori* probabilities, $\eta_i = 1/3$, and overlaps $s_1 = 0.5$ and $s_2 = 0.3$. States with $0 \leq s_3 \leq 0.976$ are LI. For $s_1 s_2 \leq s_3 \leq s_2/s_1$

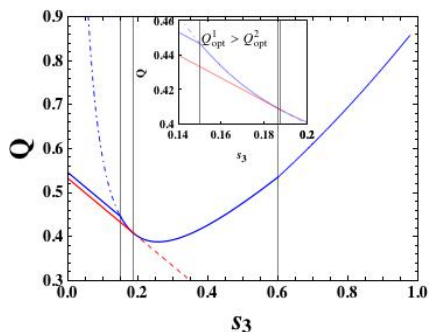


FIG. 4: $Q_{opt}^{(1)}$ (blue) and $Q_{opt}^{(2)}$ (red) vs. s_3 for $\eta_i = 1/3$, $s_1 = 0.5$ and $s_2 = 0.3$. At the branch point $s_3 = 0.1875$ the two curves have the same slope. Both curves are extended beyond their range (dotted lines).

($0.15 \leq s_3 \leq 0.6$) all $q_i < 1$ and $Q_{opt}^{(1)}$ exists. The condition $\Delta_{ij} \geq 0$ gives the range $0 < s_3 \leq 0.1875$ for $Q_{opt}^{(2)}$. In this range, $Q_{opt}^{(2)}$ is optimal for the discrimination of all three states. At the branch point $s_3 = 0.1875$ the two curves have the same slope. While $Q_{opt}^{(1)}$ is invariant under permutation of the indexes, $Q_{opt}^{(2)}$ is not. So, for $s_3 \leq 0.1875$ the symmetry is broken. For $s_3 < 0.15$ a sub-optimal solution with $q_3 = 1$ coexists with $Q_{opt}^{(2)}$. For $0.6 \leq s_3 \leq 0.976$ the edge-solution with $q_2 = 1$ is the only solution and it is also optimal.

In summary, we have developed a complete and intuitive geometric picture of the unambiguous discrimination problem that lends itself to a straightforward numerical algorithm for finding the optimal failure probabilities. In addition, we have shown that the results depend on the phases only through an invariant combination that is the Berry phase. We have also shown that the optimum measurement is either a single-valued function of the parameters or a bi-valued one, in which case it exhibits a second-order symmetry breaking phase transition-like phenomenon.

Finally, we point out that the geometric interpretation holds also for $N > 3$. Then the optimality region is a hyperbolic surface and the $Q = \text{constant}$ plane is a hyperplane in N -dimension. Their common point for the lowest possible Q is the optimal solution. It can be an internal point or it can be on one of the $N-k$ dimensional borders of the optimality region with $k = 1, \dots, N-1$. In this latter case precisely $N-k$ states can be discriminated with finite probability of success, so at least one state can always be discriminated. The dependence on the phases quickly becomes very involved; e.g., when $N = 4$ there are seven closed paths in parameter space so one needs seven geometric phases to describe the system, although only three of them are independent. Therefore, for $N > 3$ only some special cases, e.g., real and symmetric states can be treated analytically, and the best approach in the general case is numerical optimization guided by the insight gained from the geometric view.

Further details, with analytical solutions for more special cases, scaling properties, and other aspects of the geometric view are left for separate publications [19].

Acknowledgments. This research was supported by NSF Grant PHY0903660 and partial support was also provided by the Humboldt Foundation. The hospitality of and discussions with Wolfgang Schleich at the University of Ulm where much of this work was carried out and discussions with Ulrike Herzog, Georgina Olivares-Rentería and Luis Roa are also gratefully acknowledged.

-
- [1] M. A. Nielsen and I. L. Chuang, *Quantum Computation and Information* (Cambridge University Press, 2000).
- [2] J. A. Bergou, *Journal of Modern Optics* **57**, 160 (2010).
- [3] I. D. Ivanovic, *Phys. Lett. A* **123**, 257 (1987).
- [4] D. Dieks, *Phys. Lett. A* **126**, 303 (1988).
- [5] A. Peres, *Phys. Lett. A* **128**, 19 (1988).
- [6] G. Jaeger and A. Shimony, *Phys. Lett. A* **197**, 83 (1995).
- [7] A. Chefles, *Phys. Lett. A* **239**, 339 (1998).
- [8] A. Chefles, S.M. Barnett, *Phys. Lett. A* **250**, 223 (1998).
- [9] Y. Eldar, *IEEE Trans. Inf. Theory* **49**, 446 (2003).
- [10] L. Roa, C. Hermann-Avigliano, R. Salazar, and A. B. Klimov, *Phys. Rev. A* **84**, 014302 (2011).
- [11] A. Peres and D. R. Terno, *J. Phys. A* **31**, 7105 (1998).
- [12] Y. Sun, M. Hillery, and J. A. Bergou, *Phys. Rev. A* **64**, 022311 (2001).
- [13] M. A. Jafarizadeh, M. Rezaei, N. Karimi and A. R. Amiri, *Phys. Rev. A* **77**, 042314 (2008).
- [14] S. Pang and S. Wu, *Phys. Rev. A* **80**, 052320 (2009).
- [15] H. Sugimoto, T. Hashimoto, M. Horibe, and A. Hayashi, *Phys. Rev. A* **82**, 032338 (2010).
- [16] R. Bhatia, *Positive definite matrices*, Princeton Series in Applied Mathematics (Princeton University Press, 2006).
- [17] S. Pancharatnam, *Proc. Indian Acad. Sci. A* **44**, 247 (1956).
- [18] M. V. Berry, *Proc. R. Soc. Lond. A* **392**, 45 (1984).
- [19] U. Futschik, G.A. Olivares-Rentería, L. Roa, E. Feldman, J.A. Bergou, to be submitted to *Phys. Rev. A* (2012).